

A simple method for compressible multiphase mixtures and interfaces

Nikolai Andrianov¹, Richard Saurel² and Gerald Warnecke^{1,*,\dagger}

¹*IAN, Otto-von-Guericke Universität Magdeburg, PSF 4120, D-39016 Magdeburg, Germany*

²*Institut Universitaire des Systèmes Thermiques Industriels, 5 rue Enrico Fermi, 13453 Marseille Cedex 13, France and INRIA Projet SMASH, 2004 route des Lucioles, 06902 Sophia Antipolis*

SUMMARY

We develop a Godunov-type scheme for a non-conservative, unconditional hyperbolic multiphase model. It involves a set of seven partial differential equations and has the ability to solve interface problems between pure materials as well as compressible multiphase mixtures with two velocities and non-equilibrium thermodynamics (two pressures, two temperatures, two densities, etc.). Its numerical resolution poses several difficulties. The model possesses a large number of acoustic and convective waves (seven waves) and it is not easy to unwind all these waves accurately and simply. Also, the system is non-conservative, and the numerical approximations of the corresponding terms need to be provided. In this paper, we focus on a method, based on a characteristic decomposition which solves these problems in a simple way and with good accuracy. The robustness, accuracy and versatility of the method is clearly demonstrated on several test problems with exact solutions. Copyright © 2003 John Wiley & Sons, Ltd.

KEY WORDS: multiphase flow; hyperbolic model; Godunov-type scheme

1. INTRODUCTION

Multiphase flows are involved in a huge number of fundamental and industrial applications. Multiphase mixtures may have several origins. Usually they are consequences of a physical mixing process of several fluids or materials. But under some circumstances, they may come from artificial smearing of contact discontinuities separating fluids of different physical and chemical properties.

We consider here the numerical resolution of a compressible multiphase flow model, first proposed by Baer and Nunziato [1] for detonation waves in granular explosives, and modified

* Correspondence to: G. Warnecke, IAN, Otto-von-Guericke Universität Magdeburg, Fakultät für Mathematik, PSF 4120, D-39016 Magdeburg, Germany.

† E-mail: gerald.warnecke@mathematik.uni-magdeburg.de

Contract/grant sponsor: European Science Foundation (ESF)

Contract/grant sponsor: DFG-Graduiertenkolleg 'Modellierung, Berechnung und Identifikation mechanischer Systeme'

in Reference [2] for the resolution of multiphase mixtures and interface problems between pure compressible materials.

In this last reference, the goal was to use the same numerical method for the physical problems involving two-phase mixtures with two velocities, as well as interface problems with the single pressure and velocity. This aim was reached by using:

- An unconditional hyperbolic model for fluid mixtures, i.e. the system remains hyperbolic for all admissible states.
- An accurate method for flux computation as well as for the non-conservative terms.
- Pressure and velocity relaxation procedures.

This model and numerical solution procedures have been applied to several difficult physical problems like detonation waves in multiphase mixtures, multidimensional interfaces under shock interaction, underwater explosions for example and cavitation in liquids [3].

However, this method has some drawbacks. The Riemann solver used in Reference [2] and in Reference [3] was much too dissipative. It involved only two waves instead of seven. Consequently not all the waves were upwinded, and the numerical solution was not accurate enough, in particular for convective waves. Here we propose a simple way to account for these waves in the solver.

In the literature several ways of solving the system from References [1,2], which take into account all waves, can be found. One of the common approaches is to neglect the non-conservative terms in the system of governing equations. This is done e.g. in Reference [4], where the authors give the following reasons to do so. First, they note that even without the non-conservative terms the system remains consistent with the second law of thermodynamics. Then, for the applications they consider, deflagration-to-detonation transition (DDT), these terms do not play a significant role in the process. Finally, they mention that the results without non-conservative terms fit well to the experimental data. The resulting system could be then expressed in divergence form and the Roe method is used for its solution.

Another method of solving the same type of model with neglected non-conservative terms is proposed in Reference [5]. The advection equation for the volume fraction is written in conservative form, and the characteristic decomposition method with the upwinding described as follows is used to solve the system. Namely, the seven left eigenvectors are used to project into the characteristic fields, while only the first six entries of the seven right eigenvectors are used to project back out of these fields.

However, as we show in Section 3, neglecting the non-conservative terms could lead to unphysical solutions, in particular when considering interface problems between pure materials.

The methodology which we follow in this work was introduced in Reference [2]. In contrast to the methods mentioned above, we do not neglect non-conservative terms. This allows us to preserve the conditions of uniformity for pressure and velocity by construction, see Section 3.

The numerical method which we employ here for the upwinding of the convective and acoustic contributions of the flux is due to Gallouet and Masella [6]. It is based on the local resolution of the linearized Riemann problem. The numerical flux is defined following the Godunov scheme, as the physical flux at the interface value of the solution of the Riemann problem. Then the non-conservative terms are discretized following the lines of Saurel and Abgrall [2]. This approach makes use of the fact that homogeneous states in pressure and velocity should be preserved. Thus, for conservative systems, the scheme is conservative and consistent without fulfilling Roe's condition on the linearized Jacobian matrix. We do

not need to compute the Roe matrix in order to have a conservative method, which could be quite costly and cumbersome for big systems or when using complicated equations of state.

This feature is especially useful for typical problems, arising in multiphase flow modelling, where we often have to complete the seven equation model by extra equations. These could be the conservation equation for the number of particles per unit volume, which is needed for the calculation of the particle diameter, drag force, etc. We can also consider the micro–macro coupling effects like bubble pulsation, particle rotation, pore collapse, etc., see References [7, 8]. Such type of system involves more equations, but remains hyperbolic and has the same structure.

The paper is organized as follows. In Section 2, we briefly review the mathematical model. Section 3 is devoted to the discussion on the necessity of considering the non-conservative terms. Sections 4–6 describe the numerical method, and Section 7 contains some numerical examples.

2. PRESENTATION OF THE MODEL

Let us denote the gas and liquid phase with the subscripts g and l, respectively, and the interface parameters with the subscript ‘int’. Let α_k be the volume fractions, ρ_k the material densities, P_k the pressures, and $E_k = e_k + u_k^2/2$ the specific total energies for $k = g, l$. The parameters λ and μ determine the relaxation rates of velocities and pressures of the phases, see Reference [2]. In Reference [2], the following definitions are proposed for the interface pressure P_{int} and velocity V_{int} ,

$$\begin{aligned} P_{\text{int}} &= \alpha_g P_g + \alpha_l P_l \\ V_{\text{int}} &= (\alpha_g \rho_g u_g + \alpha_l \rho_l u_l) / (\alpha_g \rho_g + \alpha_l \rho_l) \end{aligned} \quad (1)$$

Other choices are possible according to the physical situation of interest. Then the governing equations for the one-dimensional compressible two-phase flow are [2]

$$\begin{aligned} \frac{\partial \alpha_g}{\partial t} + V_{\text{int}} \frac{\partial \alpha_g}{\partial x} &= \mu(P_g - P_l) \\ \frac{\partial \alpha_g \rho_g}{\partial t} + \frac{\partial \alpha_g \rho_g u_g}{\partial x} &= 0 \\ \frac{\partial \alpha_g \rho_g u_g}{\partial t} + \frac{\partial \alpha_g \rho_g u_g^2 + \alpha_g P_g}{\partial x} &= P_{\text{int}} \frac{\partial \alpha_g}{\partial x} + \lambda(u_l - u_g) \\ \frac{\partial \alpha_g \rho_g E_g}{\partial t} + \frac{\partial \alpha_g u_g (\rho_g E_g + P_g)}{\partial x} &= P_{\text{int}} V_{\text{int}} \frac{\partial \alpha_g}{\partial x} + \lambda(u_l - u_g) V_{\text{int}} - \mu P_{\text{int}} (P_g - P_l) \\ \frac{\partial \alpha_l \rho_l}{\partial t} + \frac{\partial \alpha_l \rho_l u_l}{\partial x} &= 0 \\ \frac{\partial \alpha_l \rho_l u_l}{\partial t} + \frac{\partial \alpha_l \rho_l u_l^2 + \alpha_l P_l}{\partial x} &= -P_{\text{int}} \frac{\partial \alpha_g}{\partial x} - \lambda(u_l - u_g) \end{aligned} \quad (2)$$

$$\frac{\partial \alpha_1 \rho_1 E_1}{\partial t} + \frac{\partial \alpha_1 u_1 (\rho_1 E_1 + P_1)}{\partial x} = -P_{\text{int}} V_{\text{int}} \frac{\partial \alpha_g}{\partial x} - \lambda (u_1 - u_g) V_{\text{int}} + \mu P_{\text{int}} (P_g - P_1)$$

Equations (2) are closed by two equations of state (EOS), here we use the *stiffened gas EOS*, and the saturation constraint for the volume fractions

$$\begin{aligned} P_k &= (\gamma_k - 1) \rho_k e_k - \gamma_k \pi_k \\ \alpha_g + \alpha_1 &= 1 \end{aligned} \quad (3)$$

where γ_k and π_k are constants, specific for each phase. For gas we take $\gamma_g = 1.4$, $\pi_g = 0$, for liquid $\gamma_l = 4.4$, $\pi_l = 6 \times 10^8$ Pa. Any other convex equation of state may be used for the thermodynamical closure of the model.

In order to investigate the mathematical structure of (2) it is convenient to rewrite it in primitive variables,

$$\frac{\partial \mathbf{W}}{\partial t} + \mathbf{A} \frac{\partial \mathbf{W}}{\partial x} = \mathbf{S} \quad (4)$$

where

$$\mathbf{W} = (\alpha_g, \rho_g, u_g, P_g, \rho_l, u_l, P_l) \quad (5)$$

the vector \mathbf{S} contains the non-differential source terms, and the matrix \mathbf{A} is given as

$$\mathbf{A} = \begin{pmatrix} V_{\text{int}} & 0 & 0 & 0 & 0 & 0 & 0 \\ \frac{\rho_g}{\alpha_g} (u_g - V_{\text{int}}) & u_g & \rho_g & 0 & 0 & 0 & 0 \\ \frac{P_g - P_{\text{int}}}{\alpha_g \rho_g} & 0 & u_g & 1/\rho_g & 0 & 0 & 0 \\ \frac{\rho_g c_{\text{int},g}^2}{\alpha_g} (u_g - V_{\text{int}}) & 0 & \rho_g c_g^2 & u_g & 0 & 0 & 0 \\ -\frac{\rho_l}{\alpha_1} (u_l - V_{\text{int}}) & 0 & 0 & 0 & u_l & \rho_l & 0 \\ -\frac{P_l - P_{\text{int}}}{\alpha_1 \rho_l} & 0 & 0 & 0 & 0 & u_l & 1/\rho_l \\ -\frac{\rho_l c_{\text{int},l}^2}{\alpha_1} (u_l - V_{\text{int}}) & 0 & 0 & 0 & 0 & \rho_l c_l^2 & u_l \end{pmatrix} \quad (6)$$

where

$$c_k^2 = \frac{p_k / \rho_k^2 - \partial e_k / \partial \rho_k |_{p_k}}{\partial e_k / \partial p_k |_{\rho_k}} \quad \text{and} \quad c_{\text{int},k}^2 = \frac{P_{\text{int}} / \rho_k^2 - \partial e_k / \partial \rho_k |_{p_k}}{\partial e_k / \partial p_k |_{\rho_k}}$$

are the sound speeds for the phase k and for the phase k at the interface, respectively. A straightforward computation gives us the following expressions for the seven eigenvalues

$$\begin{aligned} \lambda_1 &= V_{\text{int}} \\ \lambda_2 &= u_g + c_g, \quad \lambda_3 = u_g - c_g, \quad \lambda_4 = u_g \\ \lambda_5 &= u_l + c_l, \quad \lambda_6 = u_l - c_l, \quad \lambda_7 = u_l \end{aligned} \quad (7)$$

The corresponding right eigenvectors are

$$\mathbf{r}_1 = \begin{bmatrix} \alpha_g \alpha_1 \sigma_1 \sigma_2 \\ -\alpha_1 \sigma_2 (\rho_g (\sigma_1 - c_{\text{int},g}^2) + P_g - P_{\text{int}}) \\ \alpha_1 \sigma_2 (u_g - V_{\text{int}}) (P_g - P_{\text{int}} - \rho_g c_{\text{int},g}^2) / \rho_g \\ \alpha_1 \sigma_2 (\rho_g c_{\text{int},g}^2 (u_g - V_{\text{int}})^2 - c_g^2 (P_g - P_{\text{int}})) \\ -\alpha_g \sigma_1 (\rho_l (c_{\text{int},l}^2 - \sigma_2) - P_l + P_{\text{int}}) \\ \alpha_g \sigma_1 (u_l - V_{\text{int}}) (-P_l + P_{\text{int}} + \rho_l c_{\text{int},l}^2) / \rho_l \\ \alpha_g \sigma_1 (-\rho_l c_{\text{int},l}^2 (u_l - V_{\text{int}})^2 + c_l^2 (P_l - P_{\text{int}})) \end{bmatrix} \quad (8)$$

$$\mathbf{r}_2 = \begin{bmatrix} 0 \\ \rho_g \\ c_g \\ \rho_g c_g^2 \\ 0 \\ 0 \\ 0 \end{bmatrix}, \quad \mathbf{r}_3 = \begin{bmatrix} 0 \\ \rho_g \\ -c_g \\ \rho_g c_g^2 \\ 0 \\ 0 \\ 0 \end{bmatrix}, \quad \mathbf{r}_4 = \begin{bmatrix} 0 \\ 1 \\ 0 \\ 0 \\ 0 \\ 0 \\ 0 \end{bmatrix} \quad (9)$$

$$\mathbf{r}_5 = \begin{bmatrix} 0 \\ 0 \\ 0 \\ 0 \\ \rho_l \\ c_l \\ \rho_l c_l^2 \end{bmatrix}, \quad \mathbf{r}_6 = \begin{bmatrix} 0 \\ 0 \\ 0 \\ 0 \\ \rho_l \\ -c_l \\ \rho_l c_l^2 \end{bmatrix}, \quad \mathbf{r}_7 = \begin{bmatrix} 0 \\ 0 \\ 0 \\ 0 \\ 1 \\ 0 \\ 0 \end{bmatrix} \quad (10)$$

where

$$\sigma_1 = c_g^2 - (u_g - V_{\text{int}})^2, \quad \sigma_2 = c_l^2 - (u_l - V_{\text{int}})^2$$

Therefore, system (2) is hyperbolic, wherever the eigenvectors are linearly independent. Note that system (2) is not strictly hyperbolic. Indeed, situations are possible, when some of the eigenvalues of the gas phase can coincide with some of the liquid phase. Moreover, it is easy to see that the eigenvectors (8)–(10) become linearly dependent in the points in the flow, where any one of conditions

$$\alpha_g = 0, \quad \alpha_l = 0, \quad \sigma_1 = 0, \quad \text{or} \quad \sigma_2 = 0$$

holds.

In this work we do not consider the mass and convective heat transfer terms, which have no importance for the design of the hyperbolic solver. The reader is referred to Reference [3] for a description of such terms.

Note that the hyperbolicity of the model is only a consequence of the compressibility of the fluids. One can consider other assumptions on the interface parameters (1) without losing hyperbolicity.

3. WHY ARE THE NON-CONSERVATIVE TERMS IMPORTANT

We wish to show the importance of the non-conservative terms by using the following physical principle due to Reference [9]: a flow, uniform in velocity and pressure, must remain uniform during its temporal evolution. In other words, under the uniformity conditions on velocity and pressure, a contact discontinuity must be preserved.

Consider the mass and momentum conservation equations for one of the phases, we omit the subscript g or l for brevity,

$$\begin{aligned} \frac{\partial \alpha \rho}{\partial t} + \frac{\partial \alpha \rho u}{\partial x} &= 0 \\ \frac{\partial \alpha \rho u}{\partial t} + \frac{\partial \alpha \rho u^2 + \alpha P}{\partial x} &= \delta P_{\text{int}} \frac{\partial \alpha}{\partial x} \end{aligned} \quad (11)$$

Here the parameter $\delta = 1$ for our model and $\delta = 0$ for the models with neglected non-conservative terms [4, 5]. Let us show that with the second choice of δ the system does not preserve contact discontinuities.

Indeed, differentiating (11) out, we have

$$\begin{aligned} \frac{\partial \alpha \rho}{\partial t} + u \frac{\partial \alpha \rho}{\partial x} + \alpha \rho \frac{\partial u}{\partial x} &= 0 \\ u \frac{\partial \alpha \rho}{\partial t} + \alpha \rho \frac{\partial u}{\partial t} + u^2 \frac{\partial \alpha \rho}{\partial x} + \alpha \rho \frac{\partial u^2}{\partial x} + P \frac{\partial \alpha}{\partial x} + \alpha \frac{\partial P}{\partial x} &= \delta P_{\text{int}} \frac{\partial \alpha}{\partial x} \end{aligned}$$

Using the assumption of the uniform velocity and pressure field and the estimates (1), we get

$$\begin{aligned} P_{\text{int}} &= P, \quad V_{\text{int}} = u \\ \frac{\partial \alpha \rho}{\partial t} + u \frac{\partial \alpha \rho}{\partial x} &= 0 \end{aligned} \quad (12)$$

$$\begin{aligned} \frac{\partial P}{\partial x} &= 0 \\ \frac{\partial u}{\partial x} &= 0 \end{aligned} \quad (13)$$

This implies that

$$\alpha \rho \frac{\partial u}{\partial t} + P \frac{\partial \alpha}{\partial x} = \delta P \frac{\partial \alpha}{\partial x}$$

It appears clearly that in order for the flow to remain uniform with respect to velocity, i.e.

$$\frac{\partial u}{\partial t} = 0 \tag{14}$$

it is necessary that

$$\delta = 1$$

The assumption $\delta = 0$ is valid only in the particular and very restrictive case of

$$\frac{\partial \alpha}{\partial x} = 0$$

Consider now the energy equation, to check that the pressure evolution is zero too,

$$\frac{\partial \alpha \rho E}{\partial t} + \frac{\partial u(\alpha \rho E + \alpha P)}{\partial x} = \delta P_{\text{int}} V_{\text{int}} \frac{\partial \alpha}{\partial x}$$

Differentiating out and using the uniformity of velocity and pressure, we get

$$\alpha \rho \frac{\partial E}{\partial t} + \alpha \rho u \frac{\partial E}{\partial x} + Pu \frac{\partial \alpha}{\partial x} = \delta Pu \frac{\partial \alpha}{\partial x} \tag{15}$$

By (14) one has

$$\frac{\partial E}{\partial t} = \frac{\partial e}{\partial t}$$

so (15) becomes

$$\alpha \rho \frac{de}{dt} + Pu \frac{\partial \alpha}{\partial x} = \delta Pu \frac{\partial \alpha}{\partial x}$$

where $d/dt = \partial/\partial t + u\partial/\partial x$. Since $e = e(P, \rho)$,

$$\frac{de}{dt} = \left. \frac{\partial e}{\partial P} \right|_{\rho} \frac{dP}{dt} + \left. \frac{\partial e}{\partial \rho} \right|_P \frac{d\rho}{dt}$$

and by (13),

$$\frac{de}{dt} = \left. \frac{\partial e}{\partial P} \right|_{\rho} \frac{\partial P}{\partial t} + \left. \frac{\partial e}{\partial \rho} \right|_P \frac{d\rho}{dt}$$

Using the advection equation for the volume fraction

$$\frac{\partial \alpha}{\partial t} + u \frac{\partial \alpha}{\partial x} = 0$$

and the continuity equation (12) we get

$$\frac{\partial \rho}{\partial t} + u \frac{\partial \rho}{\partial x} = 0$$

so that

$$\frac{d\rho}{dt} = 0$$

hold. The energy equation becomes

$$\alpha\rho \left. \frac{\partial e}{\partial P} \right|_{\rho} \frac{\partial P}{\partial t} + Pu \frac{\partial \alpha}{\partial x} = \delta Pu \frac{\partial \alpha}{\partial x}$$

which states again that

$$\frac{\partial P}{\partial t} = 0$$

only if

$$\delta = 1$$

Thus, the flow remains uniform with respect to the velocity and pressure only when the non-conservative terms are considered.

Note that though in the case of a discontinuous flow the classical derivatives used in this section are not defined, we can get the preceding result in the sense of distributions. See Schwartz [10] for the general theory of distributions. Indeed, assuming the velocity and pressure fields to be uniform, we can rewrite system (11) in a weak sense

$$\langle \phi_t, \alpha\rho \rangle + u\langle \phi_x, \alpha\rho \rangle + \int_{-\infty}^{+\infty} \phi(x,0)\alpha(x,0)\rho(x,0) dx = 0 \quad (16)$$

$$\begin{aligned} & u\langle \phi_t, \alpha\rho \rangle + u^2\langle \phi_x, \alpha\rho \rangle + \langle \phi_x, \alpha P \rangle \\ & - \langle \phi_x, \delta P\alpha \rangle + u \int_{-\infty}^{+\infty} \phi(x,0)\alpha(x,0)\rho(x,0) dx = 0 \end{aligned} \quad (17)$$

where $\phi \in C_0^1(\mathbb{R} \times [0, \infty[)$ is a test function and

$$\langle f, g \rangle = \int_0^{+\infty} \int_{-\infty}^{+\infty} fg dx dt$$

Multiplying (16) by u and subtracting the result from (17), one gets

$$\langle \phi_x, \alpha P \rangle = \langle \phi_x, \delta P\alpha \rangle$$

Using again the uniformity of pressure and the fact that the equality must hold for every ϕ , one necessarily gets that

$$\delta = 1$$

4. NUMERICAL METHOD

Following Reference [2], we use the Strang splitting technique for the numerical solution of (2):

$$\mathbf{V}_i^{n+1} = L_s^{\Delta t/2} L_h^{\Delta t} L_s^{\Delta t/2} \mathbf{V}_i^n$$

where \mathbf{V}_i^n is the vector of state variables on a mesh cell i and time t_n , i.e.

$$\mathbf{V}_i^n = (\alpha_g, \alpha_g \rho_g, \alpha_g \rho_g u_g, \alpha_g \rho_g E_g, \alpha_1 \rho_1, \alpha_1 \rho_1 u_1, \alpha_1 \rho_1 E_1)$$

L_h is the operator of numerical solution of the hyperbolic part of system (2), and L_s is the operator of integration of the source and relaxation terms. Here we focus on the hyperbolic operator; the details on relaxation procedures may be found in Reference [11].

4.1. Hyperbolic operator

The hyperbolic part of system (2) can be rewritten in the following form:

$$\frac{\partial \alpha_g}{\partial t} + V_{\text{int}} \frac{\partial \alpha_g}{\partial x} = 0 \quad (18)$$

$$\frac{\partial \mathbf{U}}{\partial t} + \frac{\partial \mathbf{f}(\mathbf{U})}{\partial x} = \mathbf{H} \frac{\partial \alpha_g}{\partial x} \quad (19)$$

where \mathbf{U} is given by

$$\mathbf{U}_i = (\alpha_g \rho_g, \alpha_g \rho_g u_g, \alpha_g \rho_g E_g, \alpha_1 \rho_1, \alpha_1 \rho_1 u_1, \alpha_1 \rho_1 E_1)$$

Following the idea of Reference [2], we want to find a discretization of the non-conservative part of (2), i.e. the transport equation for α_g (18) and the term $\mathbf{H} \partial \alpha_g / \partial x$ in (19) in such a way, that the numerical approximation to the system would preserve a contact discontinuity. Let us write down the gas-related equations of (2), omitting the subscript g , the liquid part could be considered analogously,

$$\begin{aligned} \frac{\partial \alpha}{\partial t} + V_{\text{int}} \frac{\partial \alpha}{\partial x} &= 0 \\ \frac{\partial \alpha \rho}{\partial t} + \frac{\partial \alpha \rho u}{\partial x} &= 0 \\ \frac{\partial \alpha \rho u}{\partial t} + \frac{\partial \alpha \rho u^2 + \alpha P}{\partial x} &= P_{\text{int}} \frac{\partial \alpha}{\partial x} \\ \frac{\partial \alpha \rho E}{\partial t} + \frac{\partial \alpha u (\rho E + P)}{\partial x} &= P_{\text{int}} V_{\text{int}} \frac{\partial \alpha}{\partial x} \end{aligned} \quad (20)$$

Let us denote by \mathbf{f} is the physical flux function of (20), Δ some discrete form of $\partial \alpha / \partial x$, which is still to be determined, and $\mathbf{U}^*(\mathbf{U}_j^n, \mathbf{U}_{j+1}^n)$ the value of \mathbf{U} along the line $x = x_{j+1/2}$ for the

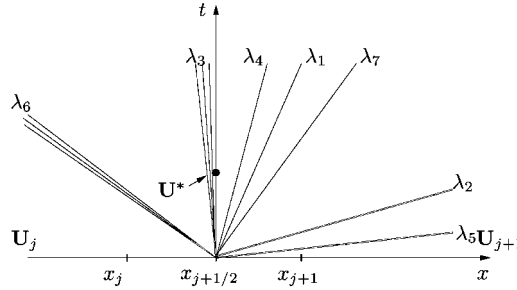


Figure 1. A typical Riemann problem, λ_i are given by (7).

Riemann problem with the states $\mathbf{U}_j^n, \mathbf{U}_{j+1}^n$, see Figure 1. Imagine we have some Godunov-type discretization of the last three equations, i.e.

$$\mathbf{U}_i^{n+1} = \mathbf{U}_i^n - \frac{\Delta t}{\Delta x} [\mathbf{f}(\mathbf{U}^*(\mathbf{U}_i^n, \mathbf{U}_{i+1}^n)) - \mathbf{f}(\mathbf{U}^*(\mathbf{U}_{i-1}^n, \mathbf{U}_i^n))] + \Delta t \mathbf{H} \Delta \tag{21}$$

Rewriting scheme (21) componentwise, we get

$$\begin{aligned} (\alpha \rho)_i^{n+1} &= (\alpha \rho)_i^n - \frac{\Delta t}{\Delta x} [(\alpha \rho u)_{i+1/2}^* - (\alpha \rho u)_{i-1/2}^*] \\ (\alpha \rho u)_i^{n+1} &= (\alpha \rho u)_i^n - \frac{\Delta t}{\Delta x} [(\alpha \rho u^2 + \alpha P)_{i+1/2}^* - (\alpha \rho u^2 + \alpha P)_{i-1/2}^*] + \Delta t (P_{\text{int}})_i^n \Delta \\ (\alpha \rho E)_i^{n+1} &= (\alpha \rho E)_i^n - \frac{\Delta t}{\Delta x} [(\alpha \rho u E + \alpha P u)_{i+1/2}^* - (\alpha \rho u E + \alpha P u)_{i-1/2}^*] + \Delta t (P_{\text{int}} V_{\text{int}})_i^n \Delta \end{aligned} \tag{22}$$

where * denotes the intermediate state.

Assume for the moment that the state \mathbf{U}^* has been determined. Then discretizations for Δ and for the transport equation of α are obtained as follows. According to the principle due to Reference [9], a flow, uniform in pressure and velocity must remain uniform in the same variables during its time evolution. In other words if we had constant pressure and velocity everywhere in a flow at the time level t_n , then we will get the same pressure and velocity at the time t_{n+1} . Substituting constant pressures and velocities in the numerical scheme (22) we get

$$\begin{aligned} u_i^n &= u_i^{n+1} = u_{i\pm 1/2}^* = V_{\text{int}} = u = \text{const} \\ P_i^n &= P_i^{n+1} = P_{i\pm 1/2}^* = P_{\text{int}} = P = \text{const} \end{aligned}$$

The first two equations of (22) will be

$$(\alpha \rho)_i^{n+1} = (\alpha \rho)_i^n - u \frac{\Delta t}{\Delta x} [(\alpha \rho)_{i+1/2}^* - (\alpha \rho)_{i-1/2}^*] \tag{23}$$

$$(\alpha \rho)_i^{n+1} u = (\alpha \rho)_i^n u - \frac{\Delta t}{\Delta x} [(\alpha \rho)_{i+1/2}^* u^2 + \alpha_{i+1/2}^* P - (\alpha \rho)_{i-1/2}^* u^2 - \alpha_{i-1/2}^* P] + \Delta t P \Delta \tag{24}$$

Multiplying (23) by u and subtracting the result from (24), we get the discretization for Δ ,

$$\Delta = \frac{1}{\Delta x}(\alpha_{i+1/2}^* - \alpha_{i-1/2}^*) \tag{25}$$

Using the definition of E and (25) in the last equation of (22), and combining it with (23), we get for internal energy

$$(\alpha\rho e)_i^{n+1} = (\alpha\rho e)_i^n - \frac{\Delta t}{\Delta x} [(\alpha\rho e)_{i+1/2}^* u - (\alpha\rho e)_{i-1/2}^* u]$$

Now using the equation of state (3) and the uniformity of pressure

$$\rho e = \frac{P + \gamma\pi}{\gamma - 1} = \text{const}$$

one gets

$$\alpha_i^{n+1} = \alpha_i^n - u \frac{\Delta t}{\Delta x} (\alpha_{i+1/2}^* - \alpha_{i-1/2}^*)$$

which is the discretized form of (18).

For the non-uniform case $u \neq \text{const}$, the Godunov-type scheme for system (18)–(19) reads

$$\alpha_i^{n+1} = \alpha_i^n - (V_{\text{int}})_i^n \frac{\Delta t}{\Delta x} (\alpha_{i+1/2}^* - \alpha_{i-1/2}^*) \tag{26}$$

$$\mathbf{U}_i^{n+1} = \mathbf{U}_i^n - \frac{\Delta t}{\Delta x} [\mathbf{f}(\mathbf{U}^*(\mathbf{U}_i^n, \mathbf{U}_{i+1}^n)) - \mathbf{f}(\mathbf{U}^*(\mathbf{U}_{i-1}^n, \mathbf{U}_i^n))] + \Delta t \mathbf{H} \Delta$$

where $\Delta = 1/\Delta x(\alpha_{i+1/2}^* - \alpha_{i-1/2}^*)$. In the following section we will specify \mathbf{U}^* , the intermediate value of the solution of the Riemann problem.

5. APPROXIMATE SOLUTION TO THE RIEMANN PROBLEM

Numerical scheme (26) requires the solution of the Riemann problem at every cell boundary at each time step. In general, the exact solution of system (2) is unknown. The determination of the Rankine–Hugoniot conditions and Riemann invariants is still an issue. Even if their expressions were known, the exact solution would be too complicated for computational purposes, so we have to use some approximate Riemann solver. The approach which we follow here is that due to Reference [6]. In this section, we give the description of the original method, and its use in the case of system (2).

5.1. Conservative systems

Consider a strictly hyperbolic system of m conservation laws

$$\mathbf{q}_t + \mathbf{g}(\mathbf{q})_x = 0, \quad \mathbf{q} = (q_1, \dots, q_m)^T \tag{27}$$

with the initial data

$$\mathbf{q}(x, 0) = \begin{cases} \mathbf{q}_l, & x \leq 0 \\ \mathbf{q}_r, & x > 0 \end{cases} \quad (28)$$

Linearizing (27), one gets

$$\mathbf{q}_t + \mathbf{B}(\bar{\mathbf{q}}(\mathbf{q}_l, \mathbf{q}_r))\mathbf{q}_x = 0 \quad (29)$$

The state $\bar{\mathbf{q}}$ is chosen in such a way, that \mathbf{B} has real eigenvalues, e.g.

$$\bar{\mathbf{q}} = \frac{\mathbf{q}_l + \mathbf{q}_r}{2}$$

For linear problem (29), the solution of the Riemann problem can be found exactly, see Reference [12] for details. We introduce the characteristic variables

$$\mathbf{s} = \mathbf{R}^{-1}\mathbf{q}, \quad \mathbf{s} = (s_1, \dots, s_m)^T$$

where \mathbf{R} is the matrix of the right eigenvectors of \mathbf{B} . Then system (27) decouples into m scalar advection equations

$$s_{it} + \lambda_i s_{ix} = 0, \quad i = 1, \dots, m$$

where λ_i are the eigenvalues of \mathbf{B} . The initial data (28) in characteristic variables will be

$$\mathbf{s}(x, 0) = \begin{cases} \mathbf{s}_l = \mathbf{R}^{-1}\mathbf{q}_l = \begin{pmatrix} s_{l1} \\ \vdots \\ s_{lm} \end{pmatrix}, & x \leq 0 \\ \mathbf{s}_r = \mathbf{R}^{-1}\mathbf{q}_r = \begin{pmatrix} s_{r1} \\ \vdots \\ s_{rm} \end{pmatrix}, & x > 0 \end{cases}$$

Thus one has

$$\begin{aligned} \mathbf{q}_r - \mathbf{q}_l &= \mathbf{R}(\mathbf{s}_r - \mathbf{s}_l) = \mathbf{R} \begin{pmatrix} s_{r1} - s_{l1} \\ \vdots \\ s_{rm} - s_{lm} \end{pmatrix} \\ &= (s_{r1} - s_{l1})\mathbf{r}_1 + \dots + (s_{r1} - s_{l1})\mathbf{r}_m = \sum_{i=1}^m b_i \mathbf{r}_i \end{aligned}$$

where $b_i = s_{ri} - s_{li}$ and \mathbf{r}_i are the right eigenvectors of \mathbf{B} . The intermediate state in the solution of Riemann problem is given by

$$\mathbf{q}^* = \mathbf{q}_l + \sum_{\lambda_i < 0} b_i \mathbf{r}_i \quad (30)$$

Then the Godunov-type scheme for conservation law (27) reads

$$\mathbf{q}_i^{n+1} = \mathbf{q}_i^n - \frac{\Delta t}{\Delta x} [\mathbf{g}(\mathbf{q}^*(\mathbf{q}_i^n, \mathbf{q}_{i+1}^n)) - \mathbf{g}(\mathbf{q}^*(\mathbf{q}_{i-1}^n, \mathbf{q}_i^n))] \tag{31}$$

The scheme is conservative and has a consistent numerical flux. Provided we use entropy-satisfying Riemann solutions \mathbf{q}^* , the weak solutions obtained by this scheme satisfy the entropy condition.

It is well known that the approximate solution of the Riemann problem, given by (30) could be non-physical (rarefaction shocks). To avoid this, the approach of Harten and Hyman [13] is used.

5.2. *Non-conservative systems*

Consider the Riemann problem for the hyperbolic part of system (2), written in the primitive variable formulation (4)–(6),

$$\frac{\partial \mathbf{W}}{\partial t} + \mathbf{A} \frac{\partial \mathbf{W}}{\partial x} = 0 \tag{32}$$

The initial conditions are

$$\mathbf{W}(x, 0) = \begin{cases} \mathbf{W}_l, & x \leq 0 \\ \mathbf{W}_r, & x > 0 \end{cases} \tag{33}$$

Following [6], we calculate the Jacobian matrix $\mathbf{A}(\bar{\mathbf{W}})$ in the average state

$$\bar{\mathbf{W}} = \frac{\mathbf{W}_l + \mathbf{W}_r}{2}$$

The intermediate state in the solution of the Riemann problem (32)–(33) is

$$\mathbf{W}^* = \mathbf{W}_l + \sum_{\lambda_i < 0} a_i \mathbf{r}_i$$

where the eigenvalues λ_i and the corresponding eigenvectors \mathbf{r}_i of the matrix $\mathbf{A}(\bar{\mathbf{W}})$ are given by (7), (8)–(10), and a_i are the coefficients of eigenvector decomposition of $\mathbf{W}_r - \mathbf{W}_l$,

$$\mathbf{W}_r - \mathbf{W}_l = \sum_{\lambda_i} a_i \mathbf{r}_i$$

For system (2) they are given by the following expressions:

$$\begin{aligned} a_1 &= \delta_1 / r_{11} \\ a_2 &= \frac{\delta_3 \rho_g c_g + \delta_4 - a_1 (r_{13} \rho_g c_g + r_{14})}{2 \rho_g c_g^2} \\ a_3 &= \frac{-\delta_3 \rho_g c_g + \delta_4 + a_1 (r_{13} \rho_g c_g - r_{14})}{2 \rho_g c_g^2} \\ a_4 &= \delta_2 - a_1 r_{12} - \rho_g (a_2 + a_3) \end{aligned}$$

$$a_5 = \frac{\delta_6 \rho_1 c_1 + \delta_7 - a_1(r_{16} \rho_1 c_1 + r_{17})}{2\rho_1 c_1^2}$$

$$a_6 = \frac{-\delta_6 \rho_1 c_1 + \delta_7 + a_1(r_{16} \rho_1 c_1 - r_{17})}{2\rho_1 c_1^2}$$

$$a_7 = \delta_5 - a_1 r_{15} - \rho_1(a_5 + a_6)$$

where r_{1k} are the components of \mathbf{r}_1 , δ_k is the k th component of $\mathbf{W}_r - \mathbf{W}_1$.

Recalculating \mathbf{W}^* into the conservative vector \mathbf{U}^* , we fully determine the Godunov-type scheme (26) for system (2).

6. EXTENSION TO THE SECOND ORDER

We use the MUSCL approach to achieve the second order, which consists of three steps, namely

- *Extrapolation:* Given piecewise-constant values \mathbf{W}_i^n , we obtain the linearly extrapolated values

$$\mathbf{W}_{i-1/2}^+ = \mathbf{W}_i^n - \frac{1}{2} \bar{\sigma}_i, \quad \mathbf{W}_{i+1/2}^- = \mathbf{W}_i^n + \frac{1}{2} \bar{\sigma}_i$$

The essential issue is that this step is performed in primitive variables; this ensures preservation of uniformity of pressure and velocity. The limited slopes $\bar{\sigma}_i$ are taken equal to

$$\bar{\sigma}_i = \begin{cases} \max[0, \min(\beta \Delta_{i-1/2}, \Delta_{i+1/2}), \min(\Delta_{i-1/2}, \beta \Delta_{i+1/2})], & \Delta_{i+1/2} > 0 \\ \min[0, \max(\beta \Delta_{i-1/2}, \Delta_{i+1/2}), \max(\Delta_{i-1/2}, \beta \Delta_{i+1/2})], & \Delta_{i+1/2} < 0 \end{cases}$$

where

$$\Delta_{i-1/2} = \mathbf{W}_i^n - \mathbf{W}_{i-1}^n, \quad \Delta_{i+1/2} = \mathbf{W}_{i+1}^n - \mathbf{W}_i^n$$

In particular, $\beta = 1$ corresponds to the minmod limiter, $\beta = 2$ to the superbee limiter.

- *Evolution:* We evolve the values of $\mathbf{W}_{i\pm 1/2}^\pm$ according to

$$\bar{\mathbf{W}}_{i-1/2}^+ = \mathbf{W}_{i-1/2}^+ - \frac{\Delta t}{2\Delta x} \mathbf{A}(\mathbf{W}_i)(\mathbf{W}_{i+1/2}^- - \mathbf{W}_{i-1/2}^+)$$

$$\bar{\mathbf{W}}_{i+1/2}^- = \mathbf{W}_{i+1/2}^- - \frac{\Delta t}{2\Delta x} \mathbf{A}(\mathbf{W}_i)(\mathbf{W}_{i+1/2}^- - \mathbf{W}_{i-1/2}^+)$$

- *The Riemann problem:* We rewrite the vectors $\bar{\mathbf{W}}_{j\pm 1/2}^\pm$ in conservative variables, solve the Riemann problems with piecewise constant data $(\bar{\mathbf{U}}_{j+1/2}^-, \bar{\mathbf{U}}_{j+1/2}^+)$ and get the intermediate states $\mathbf{U}_{j+1/2}^*$.

Then the numerical scheme (second order in space and time) reads

$$\alpha_i^{n+1} = \alpha_i^n - (V_{\text{int}})_i^n \frac{\Delta t}{\Delta x} (\bar{\alpha}_{i+1/2}^* - \bar{\alpha}_{i-1/2}^*)$$

$$\mathbf{U}_i^{n+1} = \mathbf{U}_i - \frac{\Delta t}{\Delta x} [\mathbf{f}(\mathbf{U}^*(\bar{\mathbf{U}}_{i+1/2}^-, \bar{\mathbf{U}}_{i+1/2}^+)) - \mathbf{f}(\mathbf{U}^*(\bar{\mathbf{U}}_{i-1/2}^-, \bar{\mathbf{U}}_{i-1/2}^+))] + \Delta t \mathbf{H} \Delta$$

where $\Delta = 1/\Delta x(\bar{\alpha}_{i+1/2}^* - \bar{\alpha}_{i-1/2}^*)$.

7. NUMERICAL EXAMPLES

To illustrate the properties of the new scheme we have chosen essentially the same test problems as in Reference [2]. Each problem was solved with the new scheme and with the original method of Reference [2]. In what follows, the new scheme will be referred to as VFRoe, stands for *Volumes Finis Roe* in French, notion taken from Reference [6]. The original method of Reference [2] will be referred to as HLL due to the Harten–Lax–van Leer numerical flux function used there. The calculations were made with the second-order accurate scheme using a CFL number of 0.9. The numerical results were then compared with the exact solution for the first two problems and with the experimental data for the third problem.

7.1. Water–air shock tube

We consider the shock tube filled with liquid water under high pressure at the left, and with the gas (air) at the right. Each fluid is governed by the stiffened gas EOS

$$P_k = (\gamma_k - 1)\rho_k e_k - \gamma_k \pi_k, \quad k = \text{g}, \text{l}$$

with the following parameters:

| Liquid | Gas |
|-------------------------|------------------|
| $\gamma_l = 4.4$ | $\gamma_g = 1.4$ |
| $\pi_l = 6 \times 10^8$ | $\pi_g = 0$ |

The initial conditions for system (2) are

| | | |
|--------------------------------|------------------------------|------|
| Left: $x \leq 0.7$ | Right: $x > 0.7$ | |
| $\rho_l = 1000 \text{ kg/m}^3$ | $\rho_g = 50 \text{ kg/m}^3$ | |
| $P_l = 10^9 \text{ Pa}$ | $P_g = 10^6 \text{ Pa}$ | (34) |
| $u_l = 0 \text{ m/s}$ | $u_g = 0 \text{ m/s}$ | |
| $\alpha_l = 1$ | $\alpha_g = 1$ | |

Note that at the both sides of the interface system (2) reduces to the Euler equations for liquid and gas. The solution of Riemann problem (2)–(34) is schematically depicted in Figure 2.

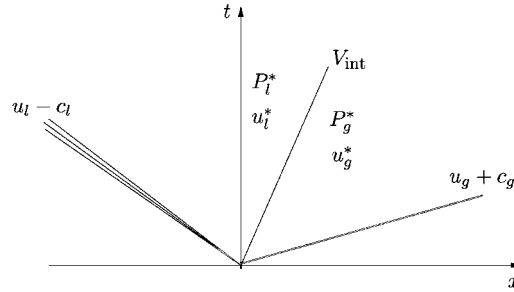


Figure 2. The Riemann problem (2)–(34). The interface $x/t = V_{\text{int}}$ separates the phases, liquid at the left and gas at the right.

Using that

$$P_g^* = P_l^*, \quad u_g^* = u_l^*$$

we can get the exact solution to the Riemann problem.

To solve it numerically, we allow the presence of a negligible small amount of gas, e.g. $\alpha_g = 10^{-8}$, at the left of the shock tube, and a small amount of water at the right. Thus the initial data will be as follows:

| | | |
|--------------------------------|--------------------------------|------|
| Left: $x \leq 0.7$ | Right: $x > 0.7$ | |
| $\rho_g = 50 \text{ kg/m}^3$ | $\rho_g = 50 \text{ kg/m}^3$ | |
| $\rho_l = 1000 \text{ kg/m}^3$ | $\rho_l = 1000 \text{ kg/m}^3$ | |
| $P_g = P_l = 10^9 \text{ Pa}$ | $P_g = P_l = 10^6 \text{ Pa}$ | (35) |
| $u_g = u_l = 0 \text{ m/s}$ | $u_g = u_l = 0 \text{ m/s}$ | |
| $\alpha_g = 10^{-8}$ | $\alpha_l = 10^{-8}$ | |

For this problem, we use both the pressure and velocity relaxation procedures. We consider the exact solution of (2)–(34) to be a reference solution for the numerical solution of (2)–(35), having in mind that we have the exact solution for the liquid at the left, and for the gas at the right.

The comparison of the numerical results for the VFRoe and HLL solvers with the exact solution at time $t = 2.2e - 4$ is presented in Figures 3–5. As expected, the VFRoe solver gives a much sharper resolution of discontinuities compared to HLL. The numerical results, obtained with the VFRoe scheme over 100 mesh cells are comparable to the results of HLL over 300 mesh cells. The calculations with 1000 mesh cells show that the shock speeds are also correctly computed.

In Figure 3, some peaks are visible in the gas parameters at the left of the interface, and in the liquid parameters to the right of it. We have observed this behaviour of the solution with the both HLL and VFRoe schemes. As mentioned before, it is not possible to fully compare these numerical results for initial data (35) with the reference solution to system (2) with initial data (34).

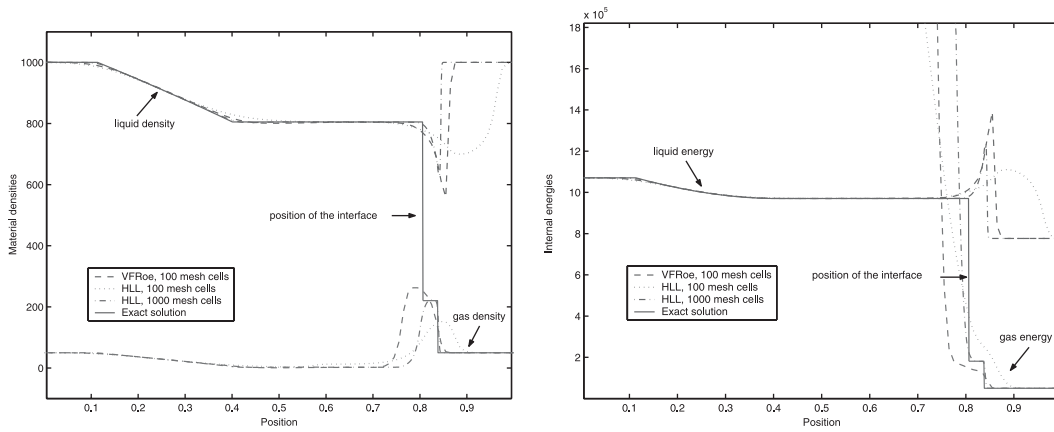


Figure 3. Water–air shock tube, material densities and energies of the phases.

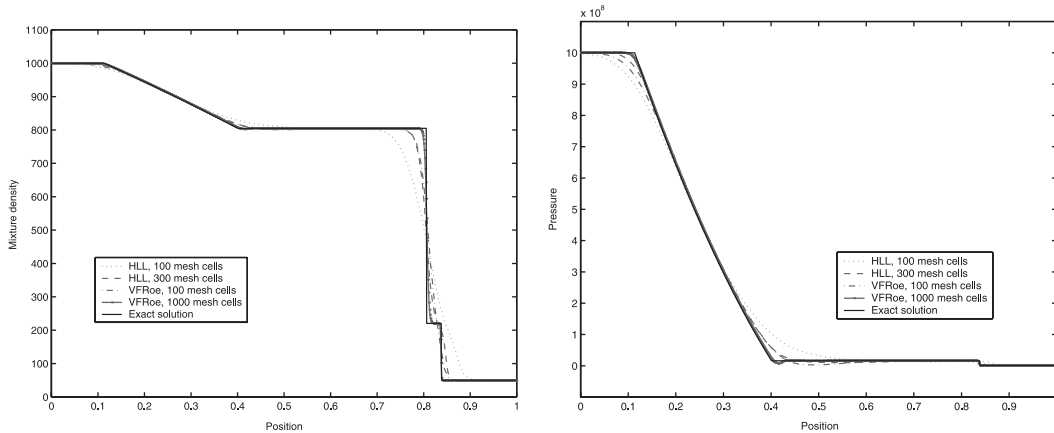


Figure 4. Water–air shock tube, mixture density and pressure.

In Figures 4–5 the distributions of the mixture density

$$\rho_{\text{mix}} = \alpha_g \rho_g + \alpha_l \rho_l$$

the relaxed pressures and velocities

$$P = P_g = P_l$$

$$u = u_g = u_l$$

and gas volume fraction α_g are presented. The reference solution for the gas volume fraction is obtained as follows. Knowing the interface velocity V_{int} from the solution of Riemann problem (2) with initial data (34), we find the displacement of the interface ΔS over the time Δt as

$$\Delta S = V_{\text{int}} \Delta t$$

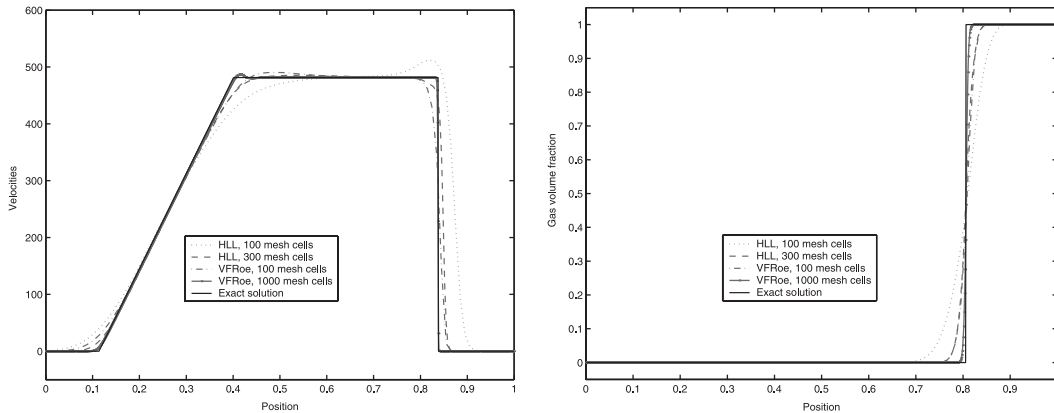


Figure 5. Water–air shock tube, velocities and gas volume fraction.

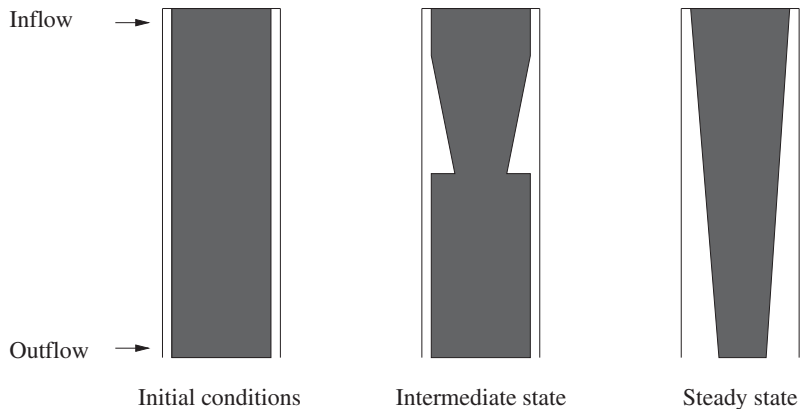


Figure 6. Water faucet problem.

In some extreme situations with very large ratios of initial pressures and densities, the VFRoe solver fails to preserve positivity of density of pressure in the intermediate state of the Riemann problem. The problem of positivity preservation of the VFRoe solver is an interesting question and will be the subject of future research.

7.2. Water faucet problem

This test, which is due to Reference [14], consists of a vertical tube 12 m in length, which contains a liquid (water) column, surrounded by gas (air). At the top, the volume fractions and the liquid velocity are given, and the gas velocity is zero. The bottom is open to atmospheric conditions. Under the action of gravity, a narrowing of the liquid jet takes place. Several stages of the process are depicted in Figure 6.

The initial conditions are as follows:

| Liquid | Gas | |
|--------------------------------|-----------------------------|------|
| $\rho_l = 1000 \text{ kg/m}^3$ | $\rho_g = 1 \text{ kg/m}^3$ | |
| $P_l = 10^5 \text{ Pa}$ | $P_g = 10^5 \text{ Pa}$ | (36) |
| $u_l = 10 \text{ m/s}$ | $u_g = 0 \text{ m/s}$ | |
| $\alpha_l = 0.8$ | $\alpha_g = 0.2$ | |

The boundary conditions are

| | Liquid | Gas | |
|------------------|---------------------------------------|-------------------------|------|
| | $u_l = 10 \text{ m/s}$ | $u_g = 0 \text{ m/s}$ | |
| Top (inflow) | $\alpha_l = 0.8$ | $\alpha_g = 0.2$ | (37) |
| | $P_l = 10^5 \text{ Pa}$ | $P_g = 10^5 \text{ Pa}$ | |
| Bottom (outflow) | α_l, α_g are extrapolated | | |

other flow variables are found by the solution of the boundary Riemann problem for the phases at the top and at the bottom of the tube.

Under the assumption that the liquid is incompressible and the pressure variation in gas is zero, one can get the exact solution for the evolution of the gas volume fraction

$$\alpha_g(x, t) = \begin{cases} 1 - \frac{(1 - \alpha_g^0)u_l^0}{\sqrt{2gx + (u_l^0)^2}}, & x \leq u_l^0 t + \frac{gt^2}{2} \\ 0.2 & \text{otherwise} \end{cases}$$

where α_g^0 is the initial gas volume fraction, u_l^0 the initial liquid velocity, g the gravity acceleration, see e.g. Reference [15]. For the numerical solution of the problem, the parameters of the stiffened gas EOS were taken as follows:

| Liquid | Gas |
|-------------------------|------------------|
| $\gamma_l = 4.4$ | $\gamma_g = 1.4$ |
| $\pi_l = 6 \times 10^6$ | $\pi_g = 0$ |

For this problem, the velocity relaxation was not used, because the phases have two distinct velocities. The comparison of the numerical results with the exact solution is presented in Figure 7.

Again, the VFRoe solver gives better results compared to that of HLL solver. The resolution of the discontinuity in gas volume fraction is not perfect, which is due to the following reasons. The sound speed in the liquid is much higher than that of the gas, so one has to choose very

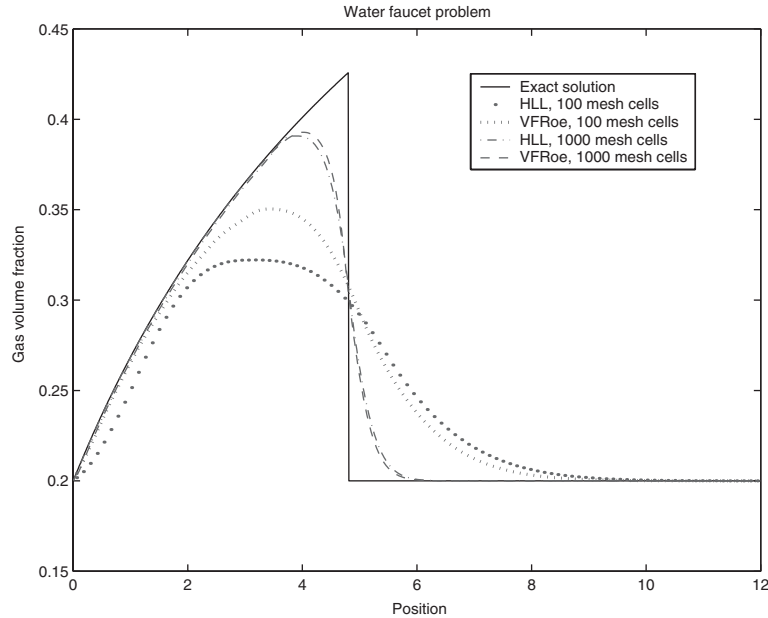
Figure 7. Water faucet problem: gas volume fraction at $t = 0.4$.

Table I. Thermodynamic constants for selected materials.

| | γ | $\pi, 10^9 \text{ Pa}$ |
|--------|----------|------------------------|
| Copper | 4.22 | 32.32 |
| Zinc | 4.17 | 15.71 |
| Epoxy | 2.94 | 3.21 |
| Spinel | 1.62 | 141.45 |

small time steps in order to satisfy the CFL condition, which leads to numerical inaccuracies. Secondly, the gas pressure is not always constant along the tube, which causes a gas flow in the negative direction and thus smearing of the interface.

7.3. Mixture Hugoniot test problem

7.3.1. Description. Consider a two-phase mixture, where each component k is governed by the stiffened gas EOS

$$P_k = (\gamma_k - 1)\rho_k e_k - \gamma_k \pi_k, \quad k = 1, 2$$

In this test, we are interested in mixtures of solid materials, which can be considered as compressible under high pressures. One can determine the constants γ_k, π_k for some materials from Reference [16]. The corresponding values are summarized in Table I.

Consider a shock wave propagating in two-phase mixtures of copper/zinc (brass) and epoxy/spinel. Using the constants from Table I, we can calculate the shock speed in the

Table II. Thermodynamic constants for selected mixtures.

| | Γ | $\Pi, 10^9 \text{ Pa}$ |
|---------------------|----------|------------------------|
| Brass (copper/zinc) | 4.20 | 27.49 |
| Epoxy/Spinel | 2.04 | 77.85 |

mixtures of solids with the two-phase flow model and the numerical method described previously. This shock speed can also be estimated from the Rankine–Hugoniot conditions of the mixture Euler equations closed by an appropriate equation of state. Such type of mixture equation of state is described in Reference [8]. Both numerical results are compared with the experimental data of Reference [16].

7.3.2. Two-phase-flow model. There are no classical Rankine–Hugoniot conditions for system (2), so we cannot find the shock speed analytically. The approach we use here is straightforward. We calculate the shock speed as the ratio of the biggest (and the only one, in case of a single shock wave) pressure gradient displacement over the time interval.

7.3.3. Euler equations coupled with the mixture EOS. For the Euler equations, we can find the shock speed analytically from the Rankine–Hugoniot jump relations. To close the system, we use the mixture EOS due to Reference [8]. It is based on the conservation of the energy and mass of the mixture, and on the equality of pressures between phases. It reads

$$P = (\Gamma - 1)\rho e - \Gamma \Pi$$

where ρ is the mixture density, e the mixture internal energy

$$\Gamma = 1 + \frac{1}{\alpha_1/(\gamma_1 - 1) + \alpha_2/(\gamma_2 - 1)}, \quad \Pi = \frac{\Gamma - 1}{\Gamma} \left(\alpha_1 \frac{\gamma_1 \pi_1}{\gamma_1 - 1} + \alpha_2 \frac{\gamma_2 \pi_2}{\gamma_2 - 1} \right)$$

and $\alpha_k, \gamma_k, \pi_k$ are the volume fractions and the thermodynamic constants for the phase $k = 1, 2$. The constants Γ, Π for the mixtures copper/zinc and epoxy/spinel are given in Table II.

7.3.4. Numerical results. Consider the two sets of initial data for the copper/zinc mixture (brass)

| | |
|--------------------------------|--------------------------------|
| Copper | Zinc |
| $\rho_1 = 8924 \text{ kg/m}^3$ | $\rho_2 = 7139 \text{ kg/m}^3$ |
| $P_1 = 10^5 \text{ Pa}$ | $P_2 = 10^5 \text{ Pa}$ |
| $u_1 = 0 \text{ m/s}$ | $u_2 = 0 \text{ m/s}$ |
| $\alpha_1 = 0.71$ | $\alpha_2 = 1 - \alpha_1$ |

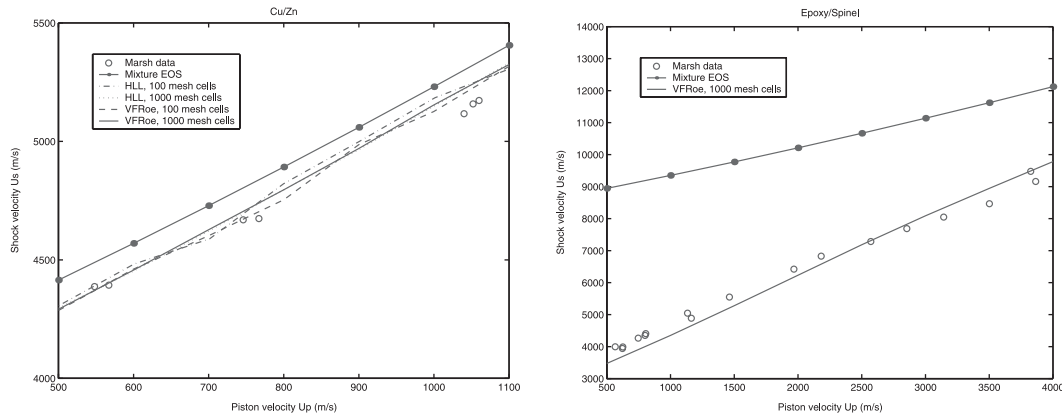


Figure 8. Mixture Hugoniot problem.

and the epoxy/spinel mixture

| Epoxy | Spinel |
|--------------------------------|--------------------------------|
| $\rho_1 = 1185 \text{ kg/m}^3$ | $\rho_2 = 3622 \text{ kg/m}^3$ |
| $P_1 = 10^5 \text{ Pa}$ | $P_2 = 10^5 \text{ Pa}$ |
| $u_1 = 0 \text{ m/s}$ | $u_2 = 0 \text{ m/s}$ |
| $\alpha_1 = 0.595$ | $\alpha_2 = 1 - \alpha_1$ |

We use a piston boundary condition on the left side to initiate the shock wave. The comparison of the calculated shock speed U_s as a function of piston velocity U_p with the experimental data of Reference [16] is presented in Figure 8.

The two-phase flow model gives a very good prediction of the shock speed even on 100 mesh cells compared to the Euler equations for the mixture. Note that the two-phase model does not need any empirically determined parameter. Only the pure material equations of state are used, in conjunction with the hyperbolic solver and relaxation procedures. The results of the VFRoe and HLL solvers do not differ qualitatively on 100 mesh cells. They both show some slight deviations from the experimental results. This is due to the non-accurate way of determining the shock speed for the two-phase flow model. Nevertheless, the results with 1000 cells show an excellent agreement with the experimental data.

8. CONCLUSIONS

In this study, we propose a simple method for compressible two-phase flows. The diffusive Riemann solver used in Reference [2] has been replaced with a more accurate one. The corresponding discretizations of the non-conservative terms have been developed in the absence of pressure or velocity jumps at the volume fraction discontinuity. The comparison of numerical results shows better resolution of the flow discontinuities, obtained by the new scheme.

The model and method are validated over several test problems with exact or experimental solutions.

ACKNOWLEDGEMENTS

The first author gratefully acknowledges the possibility of participating in the summer school CEM-RACS'2000 in Marseille and thanks the European Science Foundation (ESF) for the financial support of his stay at the IUSTI, Marseille. He was also partially funded by the DFG-Graduiertenkolleg 'Modellierung, Berechnung und Identifikation mechanischer Systeme,' Magdeburg, Germany.

REFERENCES

1. Baer MR, Nunziato JW. A two-phase mixture theory for the deflagration-to-detonation transition (DDT) in reactive granular materials. *International Journal of Multiphase Flow* 1986; **12**:861–889.
2. Saurel R, Abgrall R. A multiphase Godunov method for compressible multifluid and multiphase flows. *Journal of Computational Physics* 1999; **150**:425–467.
3. Saurel R, LeMetayer O. A multiphase model for compressible flows with interfaces, shocks, detonation waves and cavitation. *Journal of Fluid Mechanics* 2001; **431**:239–271.
4. Gonthier K, Powers J. A high-resolution numerical method for a two-phase model of deflagration-to detonation transition. *Journal of Computational Physics* 2000; **163**:376–433.
5. Fedkiw R, Merriman B, Osher S. Simplified discretization of systems of hyperbolic conservation laws containing advection equations. *Journal of Computational Physics* 2000; **157**:302–326.
6. Gallouet T, Masella JM. Un schéma de Godunov approché. *Comptes Rendus de l' Academie des Sciences Paris Séries I* 1996; **323**:77–84.
7. Gavriluk S, Saurel R. A compressible multiphase flow model with microinertia. *Journal of Computational Physics* 2002; **175**:326–360.
8. Massoni J, Saurel R, Nkonga B, Abgrall R. Proposition de méthodes et modèles Eulériens pour les problèmes à interfaces entre fluides compressibles en présence de transfert de chaleur. *International Journal of Heat and Mass Transfer* 2002; **45**:1287–1307.
9. Abgrall R. How to prevent pressure oscillations in multicomponent flow calculations: a quasi conservative approach. *Journal of Computational Physics* 1996; **125**:150–160.
10. Schwartz L. *Théorie des Distributions*. Hermann: Paris, 1966.
11. Lallemand M-H, Saurel R. Pressure relaxation procedures for multiphase compressible flows. *INRIA Rapport de recherche No. 4038*, available online at <http://www.inria.fr/rrrt/rr-4038.html>.
12. LeVeque RJ. *Numerical Methods for Conservation Laws*. Birkhäuser Verlag: Basel, 1992.
13. Harten A, Hyman JM. Self-adjusting grid methods for one-dimensional hyperbolic conservation laws. *Journal of Computational Physics* 1983; **50**:235–269.
14. Ransom VH. Numerical benchmark tests. In *Multiphase Science and Technology*, vol. 3, Hewitt GF, Delhaye JM, Zuber N (eds). Hemisphere: Washington, 1987.
15. Coquel F, El Amine K, Godlewski E, Perthame B, Rascle P. A numerical method using upwind schemes for the resolution of two-phase flows. *Journal of Computational Physics* 1997; **136**:272–288.
16. Marsh SP. *LASL Shock Hugoniot Data*. University of California Press: Berkeley, 1980.